

WAVE DRAG OF BODIES OF REVOLUTION IN UNSTEADY TRANSONIC FLOW

M. A. Naida and A. S. Fonarev

UDC 533.6.011

Determination of the wave drag of bodies is a difficult problem of aerodynamics in the transonic velocity range, because the conventional method of integration of the pressure distribution over the body in numerical solution of the problem using the theory of small perturbations is rather inaccurate and often even leads to negative values of the drag coefficient [1, 2]. Cole et al. [1, 2] proposed another approach to drag calculation, which is based on the integral form of the equation of momenta, and considered steady transonic flow around thin airfoils. The method is easily extended to the case of flow past wings, but cannot be applied directly to axisymmetric bodies, because of singularities due to the axial structure of the flow and also because of the absence of a linear relationship between the pressure and velocity components within the framework of the theory of small perturbations. The problem of applying the integral theorem of momenta to steady axisymmetric transonic flow around bodies was considered in [3]. The same approach was used in [4, 5] to determine the unsteady wave drag of bodies in plane transonic flow and to obtain the time dependence of the aerodynamic characteristics of an airfoil during its interaction with a gust, with a moving shock wave, etc.

This paper extends these results to the case of unsteady transonic flow around axisymmetric bodies. We solve the problem under the assumptions of the nonlinear transonic theory of small perturbations and investigate the unsteady "high-frequency" equation for the velocity potential. This equation makes it possible to consider aperiodic (in particular, jumpwise) variations of the flow parameters: sudden gusts, incoming shock waves, etc.

A formula for determination of the unsteady wave drag of bodies of revolution is obtained using the integral form of the equation of momenta. Singularities associated with the axial structure of the flow are taken into account.

A numerical algorithm, which is an extension of the alternating-direction method to the axisymmetric case, is used together with the Engquist-Osher monotone scheme to calculate unsteady transonic flow past bodies of revolution of various shapes.

1. Statement of the Problem. Let a slender body of revolution be in given steady transonic flow of an ideal gas with velocity U_∞ . At some initial moment, an unsteady perturbation occurs in the flow, for example, in the form of a horizontal gust, which instantly envelopes the body, or in the form of a weak shock wave whose front is located at some distance from the body. The unsteady flow around the body and the change in its integral aerodynamic characteristics in the transition regime must be investigated.

Since the free-stream Mach number M_∞ is close to unity, and the thicknesses of the bodies, the gust velocities, and the shock-wave intensities are small in comparison with the characteristic values of the same quantities of the problem, we can use the transonic theory of small perturbations.

Within the framework of this theory, the problem is described by the nonlinear unsteady equation for the potential φ of the disturbed velocity [6, 7]:

$$M_\infty^2 \varphi_{tt} + 2M_\infty^2 \varphi_{xt} = ((C_1 + C_2 \varphi_x) \varphi_x)'_x + \frac{1}{r} (r \varphi_r)'_r. \quad (1.1)$$

Here $C_1 = 1 - M_\infty^2$; $C_2 = -(\gamma + 1)M_\infty^2/2$; and γ is the adiabatic exponent. We locate the origin of the longitudinal axis of a cylindrical coordinate system at the center of the body; the x axis coincides with the

symmetry axis of the body and has the same direction as the velocity vector of the unperturbed free stream. The r axis is perpendicular to the x axis and forms with it a right-hand system of coordinates. All quantities in (1.1) are referred to their characteristic values with the subscript 0:

$$x_0 = r_0 = l, \quad u_0 = U_\infty, \quad t_0 = x_0/u_0, \quad \varphi_0 = u_0 x_0$$

(l is the body length). It should be noted that, in contrast to the case of plane symmetry, Eq. (1.1) has a singularity on the line of axial symmetry for $r = 0$. Because of this, the condition of zero normal velocity cannot be applied at the axis $r = 0$ in the case of axial symmetry. In this connection, we consider an equation which is obtained from (1.1) as $r \rightarrow 0$:

$$(r\varphi_r)'_r = 0 \quad (1.2)$$

and its solution $\varphi = f(x, t) \ln r + g(x, t)$ with the as yet unknown functions f and g . Let $R = R(x)$ be the shape of the streamlined body of revolution, which does not change with time. The condition of zero normal velocity is satisfied for $r = R$:

$$v = \varphi_r = \left. \frac{f(x, t)}{r} \right|_{r=R} = R'_x$$

(v is the vertical velocity component). Thus, $f(x, t) = RR'_x = S'_x/2\pi$ [$S(x)$ is the cross-sectional area of the streamlined body], and the solution of Eq. (1.2) is written as

$$\varphi = \frac{S'_x}{2\pi} \ln r + g(x, t). \quad (1.3)$$

It is seen that for $r \rightarrow 0$ solution (1.3) has a logarithmic singularity. Therefore, the boundary condition, as in the steady case [8], is given not on the axis $r = 0$ but on the surface of an imaginary cylinder with a fairly small radius r_* in the form

$$\varphi_r = S'_x/(2\pi r) \quad \text{for } r = r_*. \quad (1.4)$$

Since the problem is solved numerically in a large but finite domain, one should eliminate the possible influence of the outer boundaries on the flow field, which consists in reflecting the perturbations that reach the boundaries back into the flow. This is achieved by using special nonreflecting boundary conditions. For the "low-frequency" equation, such conditions were obtained in [9] by analyzing the asymptotic behavior of a relation that holds on the characteristic surface.

Let us consider the characteristic equation for (1.1):

$$M_\infty^2 \xi_t^2 + 2M_\infty^2 \xi_x \xi_t = C \xi_x^2 + \xi_r^2 \quad (C = |C_1 + 2C_2 \varphi_x|).$$

The general integral of this equation, which determines the characteristic surface (1.1), can be written as

$$\xi = \sqrt{\frac{x^2}{C} + r^2} - \frac{\sqrt{C}t}{M_\infty \sqrt{C + M_\infty^2}} - \frac{M_\infty x}{\sqrt{C} \sqrt{C + M_\infty^2}}.$$

We seek a relation on the characteristic surface in the form of a linear combination of the first derivatives of the potential. Assuming that $\varphi = \varphi(\xi)$, we obtain $\alpha\varphi_x + \beta\varphi_r + \sigma\varphi_t = \varphi_\xi(\alpha\xi_x + \beta\xi_r + \sigma\xi_t) = 0$, provided that

$$\alpha = -C\xi_x + M_\infty^2 \xi_t = -\frac{x}{\sqrt{\frac{x^2}{C} + r^2}}, \quad \beta = -\xi_r = -\frac{r}{\sqrt{\frac{x^2}{C} + r^2}},$$

$$\sigma = M_\infty^2 (\xi_t + \xi_x) = \frac{M_\infty^2 x}{C \sqrt{\frac{x^2}{C} + r^2}} - M_\infty \sqrt{\frac{C + M_\infty^2}{C}}.$$

Thus, the relation on the characteristic surface has the form

$$-\frac{x}{d}\varphi_x - \frac{r}{d}\varphi_r + M_\infty \left(\frac{M_\infty x}{Cd} - \sqrt{\frac{M_\infty^2 + C}{C}} \right) \varphi_t = 0, \quad d = \sqrt{\frac{x^2}{C} + r^2}.$$

The asymptotics of this expression in the limits $x \rightarrow -\infty$, $x \rightarrow \infty$, and $r \rightarrow \infty$ gives the boundary conditions at the left, right, and upper boundaries, respectively:

$$C\varphi_x - M_\infty(M_\infty - \sqrt{C + M_\infty^2})\varphi_t = 0 \quad \text{at } x \rightarrow -\infty; \quad (1.5)$$

$$C\varphi_x - M_\infty(M_\infty + \sqrt{C + M_\infty^2})\varphi_t = 0 \quad \text{at } x \rightarrow \infty; \quad (1.6)$$

$$M_\infty\varphi_r + \sqrt{C + M_\infty^2}\sqrt{C}\varphi_x = 0 \quad \text{at } r \rightarrow \infty. \quad (1.7)$$

Equation (1.1), together with boundary conditions (1.4)–(1.7), completely describes the problem of the unsteady interaction of a body with perturbations of various types in transonic flow. In the modeling of a body's entrance into a horizontal gust (instant enveloping), first a stationary solution with some fixed Mach number is found, and then the Mach number is changed instantaneously (in one time step) by a finite value. In solving the problem on interaction of the body with a shock wave, the latter is modeled by specifying a linear distribution of the potential at a sufficiently long distance from the body, where the flow is practically unperturbed. The weak shock wave given in this way at the initial moment $t = 0$, begins to propagate in accordance with the laws of gas dynamics in the flow field perturbed by the body for $t > 0$.

2. Determination of Wave Drag. The wave drag of an axisymmetric body will be calculated both by the usual method of integrating the pressure distribution over the body surface and by using the integral theorem of momenta. Within the framework of the transonic theory of small perturbations, the pressure coefficient in the axisymmetric case is found from the formula $c_p = -2u - v^2 - 2\varphi_t$.

Thus, it is necessary to know the perturbed velocity components u and v and the derivative of the potential with respect to time φ_t to determine the pressure coefficient on the body. The vertical velocity component v on the body is found from the condition of zero normal velocity. Let us use solution (1.3), which describes the potential distribution inside an imaginary cylinder of small radius r_* , to determine the horizontal velocity component and the derivative of the potential with respect to time. We assume that the initial boundary-value problem in the external domain, which is determined by Eq. (1.1) with the corresponding initial and boundary conditions (1.1)–(1.7), has already been solved, and, hence, the distribution of the disturbed velocity potential at the surface of the cylinder for $r = r_*$ for each moment is already known. Combining the solution in the internal domain

$$u = \varphi_x = \frac{S''_{xx}}{2\pi} \ln r + g_x$$

with the solution for the external domain for $r = r_*$, we have

$$u_* = \frac{S''_{xx}}{2\pi} \ln r_* + g_x, \quad g_x = u_* - \frac{S''_{xx}}{2\pi} \ln r_*.$$

Thus, the horizontal velocity component on the surface of the body is given by the expression

$$u(x, R, t) = u_* + \frac{S''_{xx}}{2\pi} \ln \frac{R}{r_*}.$$

Similarly, differentiating (1.3) with respect to time, we obtain $\varphi_t = g_t(x, t)$, from which it follows that the value of φ_t inside the cylinder does not depend on the transverse coordinate r , and, consequently, its value on the surface of the body coincides with its value on the surface of the cylinder for $r = r_*$, i.e., in accordance with the above assumption φ_t is known. The final expression for c_p on the surface of the body has the form

$$c_p = -2 \left(u_* + \frac{S''_{xx}}{2\pi} \ln \frac{R}{r_*} \right) - (R'_x)^2 - 2(\varphi_*)_t. \quad (2.1)$$

The wave drag coefficient c_x is found using (2.1) as follows:

$$c_x = 2\pi \int_{-0.5}^{0.5} c_p R R'_x dx = -4\pi \int_{-0.5}^{0.5} u_* R R'_x dx - 2\pi \int_{-0.5}^{0.5} \left(\frac{S''_{xx}}{\pi} \ln \frac{R}{r_*} + (R'_x)^2 \right) R R'_x dx - 4\pi \int_{-0.5}^{0.5} (\varphi_*)_t R R'_x dx. \quad (2.2)$$

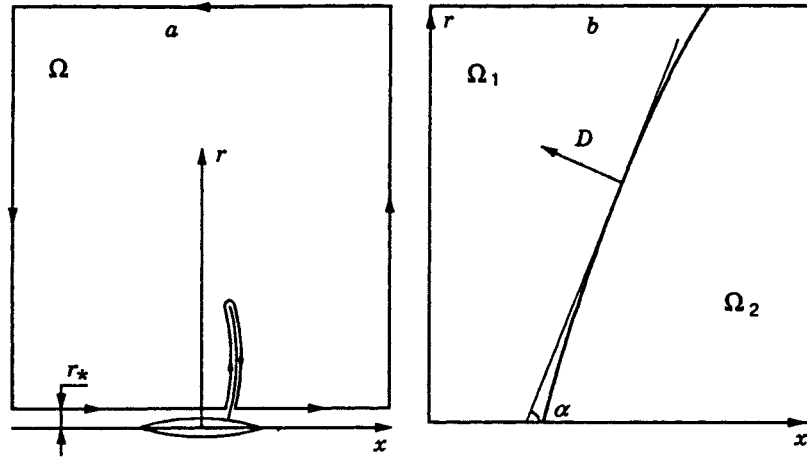


Fig. 1

It is seen that the expression for c_x consists of three terms. The second term is determined by the shape of the body and can be integrated:

$$2\pi \int_{-0.5}^{0.5} \left(\frac{S''_{xx}}{\pi} \ln \frac{R}{r_*} + (R'_x)^2 \right) R R'_x dx = \frac{(S'_x)^2}{2\pi} \ln \frac{R}{r_*} \Big|_{-0.5}^{0.5}.$$

It should be expected (in accordance with the asymptotic theory of [1]) that the contribution of the third term to c_x is insignificant in comparison with the contribution of the first term. Therefore, the method of calculation of the first term has the main influence on the accuracy of determination of c_x . As was noted, calculation of the first term in (2.2) by numerical integration over the surface of the body can lead to substantial errors, even to a negative value of the wave drag [2, 3]. In order to avoid this, we use the integral theorem of momenta and express the first term as the sum of several quadratures, which can be determined numerically without the shortcoming mentioned above. For this, we consider a system of two equations. The first of these is Eq. (1.1) and the second is an equation for the absence of vorticity in the flow:

$$rM_\infty^2 \varphi_{tt} + 2rM_\infty^2 \varphi_{xt} = (r(C_1 + C_2 \varphi_x) \varphi_x)'_x + (r\varphi_r)'_r, \quad u_r - v_x = 0.$$

Multiplying the first equation by u and the second by rv and adding them together, we obtain a relation in divergent form:

$$rM_\infty^2 (\varphi_x^2 + \varphi_x \varphi_t)'_t = r \left(C_1 \frac{u^2}{2} + \frac{2}{3} C_2 u^3 - \frac{v^2}{2} + M_\infty^2 \frac{\varphi_t^2}{2} \right)'_x + (ruv)'_r. \quad (2.3)$$

Let us integrate relation (2.3) over the calculation domain Ω (Fig. 1a) with compression shocks excluded. Applying Green's formula to the right-hand side of this relation, we have

$$\iint_{\Omega} rM_\infty^2 (\varphi_x^2 + \varphi_x \varphi_t)'_t dx dr = \int_L r \left(C_1 \frac{u^2}{2} + \frac{2}{3} C_2 u^3 - \frac{v^2}{2} + M_\infty^2 \frac{\varphi_t^2}{2} \right) dr - \int_L ruv dx \quad (2.4)$$

where L is the contour of the domain Ω . When the boundaries of the calculation domain tend to infinity, the right-hand side of (2.4) can be written as

$$I_r = \int_{sh} r \left[C_1 \frac{u^2}{2} + \frac{2}{3} C_2 u^3 - \frac{v^2}{2} + M_\infty^2 \frac{\varphi_t^2}{2} \right] dr - \int_{sh} r [uv] dx - \int_w ruv dx, \quad (2.5)$$

where the subscripts sh and w denote integration along compression shocks and along the body, respectively, and the brackets denote the difference in the enclosed quantity in passage through a shock from left to right.

Let us transform the left-hand side of relation (2.4). For this, it is necessary to take into account the

internal compression shocks moving in the domain Ω . To this end, we select domains with discontinuities and divide them into two subdomains: Ω_1 and Ω_2 (Fig. 1b). According to the calculation rules for multiple integrals and Leibnitz's formula for differentiation of parameter-dependent integrals, the left-hand side I_1 of (2.4) for the domain Ω_1 has the form

$$I_1 = \frac{d}{dt} \iint_{\Omega_1} r M_\infty^2 (\varphi_x^2 + \varphi_x \varphi_t) dx dr - \int_{sh} r M_\infty^2 (\varphi_x^2 + \varphi_x \varphi_t) \left(\frac{dx}{dt} \Big|_{sh} dr - \frac{dr}{dt} \Big|_{sh} dx \right).$$

A similar expression is obtained for the integral over the domain Ω_2 . Combining them, we find a relation for the entire domain Ω :

$$\iint_{\Omega} r M_\infty^2 (\varphi_x^2 + \varphi_x \varphi_t)'_t dx dr = \frac{d}{dt} \iint_{\Omega} r M_\infty^2 (\varphi_x^2 + \varphi_x \varphi_t) dx dr - \int_{sh} r M_\infty^2 [\varphi_x^2 + \varphi_x \varphi_t] \left(\frac{dx}{dt} \Big|_{sh} dr - \frac{dr}{dt} \Big|_{sh} dx \right). \quad (2.6)$$

In the derivation of (2.6), it was taken into account that a shock can be curvilinear (Fig. 1b). The velocity of its movement is determined by the relation

$$D = -\frac{dx}{dt} \Big|_{sh} \sin \alpha + \frac{dr}{dt} \Big|_{sh} \cos \alpha.$$

Substituting (2.5) and (2.6) into (2.4) and taking into account the condition of zero normal velocity on the body $v = R'_x$, we can express the integral over the body in terms of integrals over the shock and a multiple integral over the calculation domain:

$$\begin{aligned} \int_{-0.5}^{0.5} R R'_x u_* dx &= \int_{sh} r \left[C_1 \frac{u^2}{2} + \frac{2}{3} C_2 u^3 - \frac{v^2}{2} + M_\infty^2 \frac{\varphi_t^2}{2} \right] dr - \int_{sh} r [uv] dx \\ &+ \int_{sh} r M_\infty^2 [\varphi_x^2 + \varphi_x \varphi_t] \left(\frac{dx}{dt} \Big|_{sh} dr - \frac{dr}{dt} \Big|_{sh} dx \right) - \frac{d}{dt} \iint_{\Omega} r M_\infty^2 (\varphi_x^2 + \varphi_x \varphi_t) dx dr. \end{aligned} \quad (2.7)$$

To simplify (2.7), we use the conditions on the shock:

$$\left(-\frac{dx}{dt} \Big|_{sh} dr + \frac{dr}{dt} \Big|_{sh} dx \right) [\varphi_t + 2\varphi_x] M_\infty^2 = [C_1 u + C_2 u^2] dr + [v] dx; \quad (2.8)$$

$$[u] dx + [v] dr = 0. \quad (2.9)$$

Multiplying (2.9) by the arithmetic mean of the vertical velocity component over the shock $\langle v \rangle$, we have

$$\langle v \rangle [u] dx + \frac{[v^2]}{2} dr = 0. \quad (2.10)$$

Substituting (2.10) into (2.7), we obtain

$$\begin{aligned} \int_{-0.5}^{0.5} R R'_x u_* dx &= \int_{sh} r \left[C_1 \frac{u^2}{2} + \frac{2}{3} C_2 u^3 + M_\infty^2 \frac{\varphi_t^2}{2} \right] dr + \int_{sh} r (\langle v \rangle [u] - [uv]) dx \\ &+ \int_{sh} r M_\infty^2 [\varphi_x^2 + \varphi_x \varphi_t] \left(\frac{dx}{dt} \Big|_{sh} dr - \frac{dr}{dt} \Big|_{sh} dx \right) - \frac{d}{dt} \iint_{\Omega} r M_\infty^2 (\varphi_x^2 + \varphi_x \varphi_t) dx dr. \end{aligned} \quad (2.11)$$

We transform the expression $\langle v \rangle [u] - [uv] = -\langle u \rangle [v]$. Let us multiply (2.8) by $\langle u \rangle$:

$$-r [v] \langle u \rangle dx = -\left(\frac{dx}{dt} \Big|_{sh} dr + \frac{dr}{dt} \Big|_{sh} dx \right) r M_\infty^2 [\varphi_t + 2\varphi_x] \langle u \rangle - r [C_1 u + C_2 u^2] \langle u \rangle dr.$$

Substituting this relation into (2.11) and taking into account that

$$\frac{2}{3} [u^3] - [u^2] \langle u \rangle = \frac{[u]^3}{6}, \quad \langle u \rangle [\varphi_t] - [u \varphi_t] = -[u] \langle \varphi_t \rangle,$$

we find

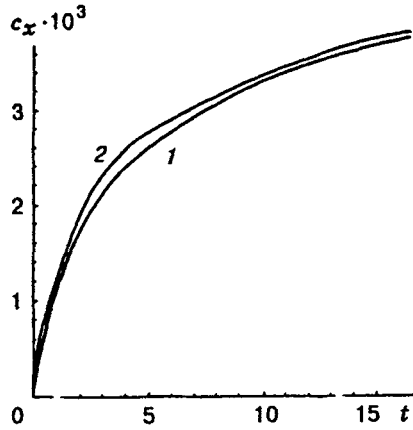


Fig. 2

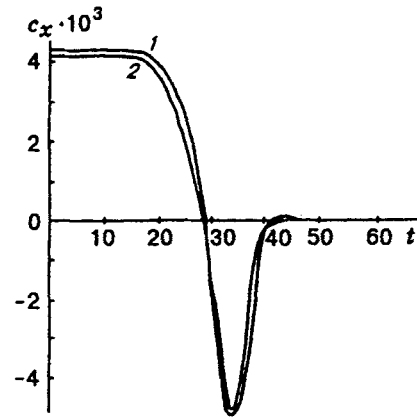


Fig. 3

$$\begin{aligned}
 \int_{-0.5}^{0.5} RR'_x u_* dx &= \int_{sh} r C_2 \frac{[u]^3}{6} dr + \int_{sh} M_\infty^2 r \frac{[\varphi_t^2]}{2} dr \\
 - \int_{sh} \left(- \frac{dx}{dt} \Big|_{sh} dr + \frac{dr}{dt} \Big|_{sh} dx \right) r M_\infty^2 [u] \langle \varphi_t \rangle &- \frac{d}{dt} \iint_{\Omega} r M_\infty^2 (\varphi_x^2 + \varphi_x \varphi_t) dx dr. \quad (2.12)
 \end{aligned}$$

Using (2.12) and (2.2), we obtain a final expression for the drag:

$$\begin{aligned}
 c_x &= 4\pi \frac{\gamma+1}{12} M_\infty^2 \int_{sh} r [\varphi_x]^3 dr - 4\pi M_\infty^2 \int_{sh} r \frac{[\varphi_t^2]}{2} dr - 4\pi M_\infty^2 \int_{sh} \frac{dx}{dt} \Big|_{sh} r \langle \varphi_t \rangle [u] dr \\
 &+ 4\pi M_\infty^2 \frac{d}{dt} \iint_{\Omega} r (\varphi_x^2 + \varphi_x \varphi_t) dx dr - 4\pi \int_{-0.5}^{0.5} (\varphi_*)_t RR'_x dx - \frac{(S'_x)^2}{2\pi} \ln \frac{R}{r_*} \Big|_{-0.5}^{0.5}. \quad (2.13)
 \end{aligned}$$

It is not necessary to transform the double integral in (2.4). Then the formula for the wave drag has the form

$$\begin{aligned}
 c_x &= 4\pi \frac{\gamma+1}{12} M_\infty^2 \int_{sh} r [\varphi_x]^3 dr + 4\pi M_\infty^2 \int_{sh} \frac{dx}{dt} \Big|_{sh} r \langle u \rangle [\varphi_t + 2\varphi_x] dr \\
 &+ 4\pi M_\infty^2 \iint_{\Omega} r \varphi_x (\varphi_t + 2\varphi_x)'_t dx dr - 4\pi \int_{-0.5}^{0.5} (\varphi_*)_t RR'_x dx - \frac{(S'_x)^2}{2\pi} \ln \frac{R}{r_*} \Big|_{-0.5}^{0.5}. \quad (2.14)
 \end{aligned}$$

It is assumed in these formulas that the position of the shock is nearly vertical, and the corresponding terms with dr/dt are omitted. Moreover, it was assumed in the derivation of the formulas that at infinity the velocity perturbations tend to zero. It should also be noted that in the case of steady axisymmetric flow, formulas (2.13) and (2.14) become the formula obtained in [3]; the first and the last terms remain.

3. Numerical Method and Calculation Results. The boundary-value problem formulated for Eq. (1.1) was solved numerically using an axisymmetric variant of the alternating-direction method developed in [3] and the Engquist-Osher monotone scheme [10]. Numerical calculations were carried out on a rectangular grid consisting of 121 nodes in the x direction and 81 nodes in the r direction. The grid was refined near the leading and trailing edges and became coarser with distance from the body. The boundaries of the calculation domain were at a distance of 30 chords from the coordinate origin in both directions. Eighty-one nodes of the calculation grid were specified on the body, which was located symmetrically about the r axis ($|x| \leq 0.5$).

To calculate the drag by the method of integration along shock waves, we developed an algorithm for

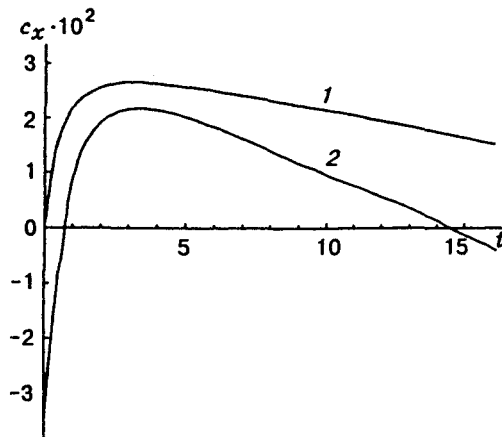


Fig. 4

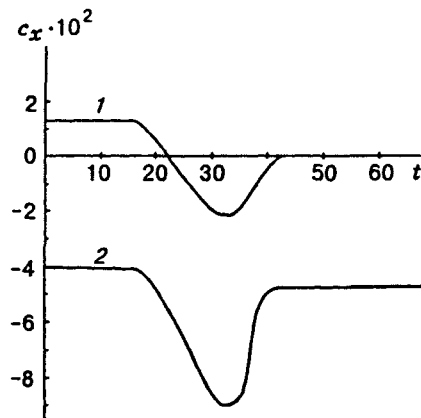


Fig. 5

their detection in each time step by abrupt decrease in the local Mach number in the flow field. If the velocity perturbations at infinity were different from zero, according to the conditions of the problem, for example, in the case of a weak plane shock wave moving with a constant nonzero perturbed velocity behind it in the half-space, this was taken into account by subtracting the corresponding constant, which was calculated for a finite domain of numerical integration, from the drag obtained by formula (2.13) or (2.14).

Let us present the results of numerical calculation of the unsteady wave drag for bodies of revolution of two types. The first type is a body formed by revolution of an arc of a circle that has 14% thickness. Let this body move at a transonic speed and enter abruptly a horizontal oncoming gust (instantaneous enveloping). In this case, the Mach number varies from $M_1 = 0.93$ to $M_2 = 0.98$. Figure 2 shows the time dependence of the unsteady drag, which varies from an essentially zero value to a value that corresponds to $M_\infty = 0.98$. Curve 1 is a drag calculation by integrating along shock waves. Here the results obtained from formulas (2.13) and (2.14) essentially coincide. Curve 2 represents a drag calculation using the usual method of integrating the pressure distribution over the surface of the body. The small difference (within 5%) observed in these two methods is caused by the fact that the body is fairly smooth and satisfies almost all assumptions of the theory of small perturbations. The local errors of the numerical calculation in the areas of the front and back points of the body are not large. A numerical calculation for the same body was performed for another problem: a plane shock wave with speed difference $\Delta u = 0.1$ approaches from behind a body moving at a transonic speed $M_\infty = 0.98$.

Figure 3 shows the time dependence of the unsteady drag as the shock wave passes over the body. Curve 1 corresponds to the calculation by integrating over shock waves, and curve 2 represents integration of the pressure distribution over the body. The difference between the curves is not large, as in the first case. It should be noted that the curves in Fig. 3 have a clearly nonmonotone character, and the drag value at some times even becomes negative. This is caused by the fact that the shock wave approaches from behind, "pushing" the body. Note the slowness of the transition process (as in the first case), which is typical of the transonic speed range. Note also that the calculations using formulas (2.13) and (2.14) again give very similar results (within 2-3%), and, therefore, we can conclude that they are equivalent from the point of view of numerical calculation of drag by the method of integrating over compression shocks.

Let us now consider the same two problems of unsteady flow around a slender body of revolution having another shape that permits local violations of the assumption in the theory of small perturbations that the derivative R'_x is small. The body consisted of three parts: a nose, which was close to an ellipsoid of revolution; a central part, which was a cylinder; and a spindle-shaped rear part. The rear part occupied half the length and the nose part occupied 30% the entire length. The nose part and central parts were smoothly

joined, as were the central part and the rear part, i.e., the derivative R'_x was continuous at these points. Flow around bodies of this type has been studied experimentally in sufficient detail by Petrov [11], who described the geometrical shape of such bodies and reported data on their wave drag. In [3], calculations of steady transonic flow around three bodies of this class were carried out, and numerical and experimental results of the wave drag were compared. The reliability of the method of drag calculation by integrating along shock waves in comparison with integration of the pressure distribution over the surface of the body is shown.

Figure 4 shows the time variation of the wave drag of the body considered for an abrupt horizontal gust (instantaneous enveloping). The initial Mach number is $M_1 = 0.93$, and after enveloping by the gust, $M_2 = 0.98$. Curve 1 illustrates the calculation by integrating along shock waves, and curve 2 represents integration of the pressure over the body. In this case (as for the steady flow regime), the difference between the curves is inadmissibly large; curve 2 does not even reach positive values of drag. At the same time, calculation curve 1 gives a result that is close to the experimental result after completion of the transition process. On the whole, the unsteady curve, unlike the curve for the first body, is nonmonotonic.

Figure 5 illustrates the time variation of the wave drag of the body considered when it is subject to the influence of a weak shock wave approaching it from behind. Curve 1 shows the calculation by integrating along compression shocks. It is nonmonotonic and has intervals of negative values (the wave pushes the body from behind) and reaches a zero value, which indicates the establishment of a new subcritical flow regime after the shock wave leaves the body and goes upstream. Curve 2 represents the result of calculation of drag by integration of the pressure distribution over the surface of the body. It is seen that this method gives negative values of the wave drag (thrust) both prior to the beginning of the interaction process and after its completion, and this suggests that the entire curve 2 is unreliable from a physical point of view.

REFERENCES

1. J. Cole and L. Cook, *Transonic Aerodynamics* [Russian translation], Mir, Moscow (1989).
2. E. M. Murman and J. D. Cole, "Inviscid drag at transonic speeds," AIAA Paper No. 74-0540 (1974).
3. M. A. Naida and A. S. Fonarev, "Effective method of calculating the wave drag of solids of revolution in the transonic range," *Prikl. Mekh. Tekh. Fiz.*, **36**, No. 3, 60-68 (1995).
4. A. S. Fonarev, "Action of wind gusts and weak shocks on an airfoil in a transonic stream," *Prikl. Mekh. Tekh. Fiz.*, **34**, No. 3, 20-27 (1993).
5. A. S. Fonarev, "Aerodynamics of wing airfoils in nonstationary transonic flows," *Russian J. Comput. Mech.*, No. 4 (1993).
6. W. J. McCroskey and P. M. Goorjian, "Interaction of airfoils with gusts and concentrated vortices in unsteady transonic flow," AIAA Paper No. 83-1691 (1983).
7. W. J. McCroskey, "The effect of gusts on the fluctuating airloads of airfoils in transonic flow," AIAA Paper No. 84-1580 (1984).
8. J. A. Krupp and E. M. Murman, "The numerical calculation of steady transonic flows past thin lifting airfoils and slender bodies," AIAA Paper No. 71-0566 (1971).
9. D. Kwak, "Nonreflecting far-field boundary conditions for unsteady transonic flow computation," *AIAA J.*, **19**, No. 11 (1981).
10. B. E. Engquist and S. J. Osher, "Stable and entropy satisfying approximations for transonic flow calculations," *Math. Comput.*, **34**, No. 19 (1980).
11. K. P. Petrov, *Aerodynamics of Aircraft Elements* [in Russian], Mashinostroenie, Moscow (1985).